

Introduction of Short and Long Range Energies To Simulate Real Chains on the 2nd Lattice

Roland F. Rapold and Wayne L. Mattice*

Maurice Morton Institute of Polymer Science, The University of Akron,
Akron, Ohio 44325-3909

Received September 11, 1995; Revised Manuscript Received December 18, 1995[⊗]

ABSTRACT: Recently, a new high-coordination lattice model for rotational isomeric state (RIS) chains was introduced, with the motivation of eventually providing a method for the more efficient simulation of dense, multichain systems by using RIS chains. Here that new method has been extended to include short and long range interaction energies, using polyethylene as the example. The short range energies were included via an extended RIS model. The classical statistical weight matrix was expanded in size and coarse-grained. The conditional probabilities derived from this extended RIS model were the basis for the probabilities of the single-bead moves used in Monte Carlo simulations on the 2nd lattice. The long range energies were introduced by using the lattice representation of the second virial coefficient. The coarse-grained linear chains have the proper mean-square dimensions, and the width of the distribution function for the squared dimensions has the proper value. Coarse-grained polyethylene macrocycles also have the proper mean-square dimensions.

Introduction

Many phenomena in polymer systems have large characteristic sizes and long relaxation times. Simple examples are the folding of proteins and the equilibration of synthetic polymer melts. The large sizes and long times make simulation of these systems infeasible with conventional methods in the all-atom representation. These shortcomings might be avoided by a reduction in the number of degrees of freedom and/or the application of more efficient methods to sample phase space. A drastic simplification occurs in lattice models. Discretization reduces the conformational space, and calculations can be carried out by using the faster integer arithmetic. In spite of considerable improvement, there is no method that achieves the simulation of specific polymers in the desired time and length scales.

As a first step toward a potential solution of this problem, we recently introduced the simulation of three simple athermal rotational isomeric state (RIS) chains on a high-coordination lattice that is a coarse-grained model of the tetrahedral lattice.¹ Since only every second site of the tetrahedral lattice is taken into account, this lattice is called the second nearest neighbor diamond lattice or 2nd lattice. The lattice is identical with the one that arises from the closest packing of uniform hard spheres. Its unit cell is a distorted cube, and the sites therefore can be treated with integer numbers. The coordination number is 12, which makes this lattice more flexible than the cubic lattice with coordination number 6. The moves of a bead within the chain are well-defined. Depending upon the vector connecting beads $i - 1$ and $i + 1$, there are 1, 2, or 4 possible locations for bead i . Simulations for single ideal chains were performed for three excluded volume restrictions: SAW (self-avoiding walk), NRRW (nonreversal random walk), and RW (random walk). The static and dynamic behavior agreed well with the expected theoretical values, confirming the ability of the designed moves to change the conformation of the chain in the expected way.

In this paper, the model is extended to include short and long range interactions. This extension will lead to the ability to treat specific polymers (instead of ideal chains) on a lattice. The only input should come from the RIS model for the real chain. Since RIS models are available for many polymers,² this extension should lead to a treatment with easy transformability. As the first and easiest model polymer, polyethylene is taken to derive and test the mapping procedure from the pure RIS description to the "universal" description on the 2nd lattice. While attention here is restricted to single chains, we note that only about 21% of the sites on the 2nd lattice would have to be filled to produce bulk density for amorphous polyethylene, using the model developed here. The relatively low occupancy of this lattice suggests that it might eventually provide an efficient route to the simulation of the amorphous polymer at bulk density.

Short Range Interactions

Preferences between the local conformations of the polymer investigated are introduced via short range interactions. Simulations with short range interactions will represent the static behavior of RIS chains. In this representation, the excluded volume restrictions are those of a nonreversal random walk, which prohibits the overlap of beads $i - 1$ and $i + 1$. All other pairs of beads can overlap. Such a simulation setup is easy to verify since the static dimensions of the classical RIS model can easily be calculated.²

Extended RIS Description. A RIS model for polyethylene is defined³ by the statistical weight matrix

$$\mathbf{U} = \begin{bmatrix} 1 & \sigma & \sigma \\ 1 & \sigma & \sigma\omega \\ 1 & \sigma\omega & \sigma \end{bmatrix} \quad (1)$$

The rows define the states of bond $i - 1$ and the columns define the states of bond i , each in the order *trans*, *gauche*⁺, *gauche*[−] (t , g^+ , g^-). The model that places the torsion angle for the g states exactly 120° from the torsion angle for t is best suited for our purpose because it most closely resembles the representation on a tetrahedral lattice. The bond angle in the RIS model introduced by Abe *et al.*³ was taken to be 112°, which is

[⊗] Abstract published in *Advance ACS Abstracts*, February 15, 1996.

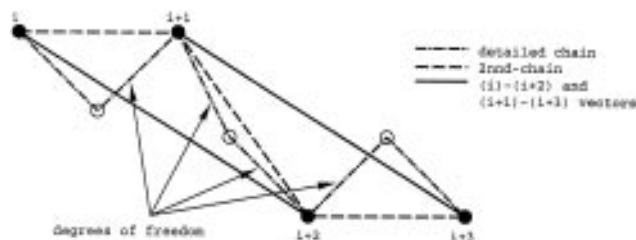


Figure 1. Two successive vectors connecting beads i and $i + 2$ and beads $i + 1$ and $i + 3$. Filled and open circles denote the chain atoms in the detailed atomistic description. The filled circles denote those atoms that are retained in the coarse-grained description on the $2nnd$ lattice.

Table 1. Lengths of Vectors Connecting Beads i and $i + 2$

| category | length (Å) | detailed conformations |
|----------|------------|--------------------------|
| A | 5.00 | tt |
| B | 4.33 | tg^+, tg^-, g^+t, g^-t |
| C | 3.53 | g^+g^+, g^-g^- |
| D | 2.50 | g^+g^-, g^-g^+ |

2.5° larger than the angle on the tetrahedral lattice. The bond length was taken as 1.53 \AA , which leads to a spacing on the $2nnd$ lattice of 2.50 \AA . The energies E_σ and E_ω were treated as empirical parameters to achieve the right characteristic ratio and the temperature dependence thereof. The suggested values were $E_\sigma = 430\text{--}590 \text{ cal/mol}$ and $E_\omega = 1700\text{--}1900 \text{ cal/mol}$. Often calculations for unperturbed polyethylene have used $E_\sigma = 0.5 \text{ kcal/mol}$ and $E_\omega = 2 \text{ kcal/mol}$. The characteristic ratio and the temperature dependence calculated with these values are close to the experimental results. Therefore, these values were taken for further use in this study.

The usual implementation of the RIS model (including this one) accounts for first- and second-order interactions. The first-order interactions depend on one degree of freedom, with the torsion angles being the only degree of freedom. First-order interactions therefore describe conformational states of three successive bonds. The second-order interactions, depending on two degrees of freedom, describe conformational states of four successive bonds. A one-to-one mapping of the RIS scheme, as represented by the statistical weight matrix shown in eq 1, onto the $2nnd$ lattice representation is not possible since the torsion angles of the respective, detailed model are not known for a coarse-grained conformation. The easiest way to categorize the conformation of a chain on the $2nnd$ lattice is by the distance between second nearest neighbor segments of the $2nnd$ lattice chain. There are four possible distances separating beads i and $i + 2$ lying between 2.50 and 5.00 \AA , as listed in Table 1. Such a segment of two virtual bonds on the $2nnd$ lattice represents a four-bond segment (two torsion angles) in the detailed, atomistic representation and corresponds to the description of n -pentane in the RIS model. Each of the different distances represents a specific set of local conformations and therefore will allow one to account for the corresponding statistical weights.

Interdependent bonds can be treated by taking account of two successive vectors of the kind just described. These vectors connect beads $(i \text{ and } i + 2)$ and $(i + 1 \text{ and } i + 3)$. Such an arrangement describes four torsion angles in the atomistic detailed model, as depicted in Figure 1, and corresponds to the description of n -heptane in the RIS model. An extension of the classical RIS model for polyethylene to consider such a six-bond unit is straightforward. The dimension of the

statistical weight matrix is increased to 9×9 :

$$\mathbf{U}^2 = \begin{bmatrix} 1 & \sigma & \sigma & \sigma & \sigma & \sigma\sigma & \sigma\sigma & \sigma\sigma\omega & \sigma\sigma\omega \\ 1 & \sigma & \sigma & \sigma & \sigma\omega & \sigma\sigma & \sigma\sigma & \sigma\sigma\omega & \sigma\sigma\omega\omega \\ 1 & \sigma & \sigma & \sigma\omega & \sigma & \sigma\sigma\omega & \sigma\sigma & \sigma\sigma\omega\omega & \sigma\sigma\omega \\ 1 & \sigma & \sigma & \sigma & \sigma & \sigma\sigma & \sigma\sigma & \sigma\sigma\omega & \sigma\sigma\omega \\ 1 & \sigma & \sigma & \sigma & \sigma & \sigma\sigma & \sigma\sigma & \sigma\sigma\omega & \sigma\sigma\omega \\ 1 & \sigma & \sigma & \sigma & \sigma\omega & \sigma\sigma & \sigma\sigma\omega & \sigma\sigma\omega & \sigma\sigma\omega\omega \\ 1 & \sigma & \sigma & \sigma\omega & \sigma & \sigma\sigma\omega & \sigma\sigma & \sigma\sigma\omega\omega & \sigma\sigma\omega \\ 1 & \sigma & \sigma & \sigma\omega & \sigma & \sigma\sigma\omega & \sigma\sigma & \sigma\sigma\omega\omega & \sigma\sigma\omega \\ 1 & \sigma & \sigma & \sigma & \sigma\omega & \sigma\sigma & \sigma\sigma\omega & \sigma\sigma\omega & \sigma\sigma\omega\omega \end{bmatrix} \quad (2)$$

The rows index the two torsion angles immediately before and after bead $i + 1$ in Figure 1, and the columns index the two torsion angles immediately before and after bead $i + 2$. The sequence of the torsional states in the rows and columns has been adjusted so that an extension to the $2nnd$ lattice model can be understood more easily. The states were grouped according to the categories described in Table 1. The sequence of the torsional states is $tt, tg^+, tg^-, g^+t, g^-t, g^+g^+, g^-g^-, g^+g^-, g^-g^+$.

Although in principle a chain on the $2nnd$ lattice can be mapped back onto the detailed representation, the accounting of the torsion angles is not retained during the simulation, and the torsional states of the detailed chain that fall into the same category as defined in Table 1 cannot be distinguished from one another. The statistical weight matrix \mathbf{U}^2 is brought to its equivalent for the coarse-grained model by substituting the statistical weights for conformations that are distinguishable for a chain on the $2nnd$ lattice. This new matrix is called $\mathbf{U}^{2'}$, and a, b , and c are the modified statistical weights that have to be assigned to obtain the coarse-grained description:

$$\mathbf{U}^{2'} = \begin{bmatrix} 1 & \sigma & \sigma & \sigma & \sigma & \sigma\sigma & \sigma\sigma & \sigma\sigma\omega & \sigma\sigma\omega \\ 1 & a & a & a & a & \sigma b & \sigma b & \sigma\omega b & \sigma\omega b \\ 1 & a & a & a & a & \sigma b & \sigma b & \sigma\omega b & \sigma\omega b \\ 1 & a & a & a & a & \sigma b & \sigma b & \sigma\omega b & \sigma\omega b \\ 1 & a & a & a & a & \sigma b & \sigma b & \sigma\omega b & \sigma\omega b \\ 1 & b & b & b & b & c & c & c\omega & c\omega \\ 1 & b & b & b & b & c & c & c\omega & c\omega \\ 1 & b & b & b & b & c & c & c\omega & c\omega \\ 1 & b & b & b & b & c & c & c\omega & c\omega \end{bmatrix} \quad (3)$$

The symmetry of the torsion potential energy function for polyethylene permits reduction of the 3×3 statistical weight matrix in eq 1 to a 2×2 statistical weight matrix, with rows and columns indexed as t and $(g^+ + g^-)$.² In a similar fashion, the 9×9 statistical weight matrix in eq 3 can be reduced to a 4×4 matrix. Here the condensed conformations are not the mirror image conformations of one another described with a symmetric torsion potential energy function, but are instead conformations of polyethylene that result in the same representation on the $2nnd$ lattice. The rows now define the category of the vectors connecting beads i and $i + 2$, and the columns define the vectors connecting beads $i + 1$ and $i + 3$, with the sequence A, B, C, D as defined in Table 1.

$$\mathbf{U}_{2nnd} = \begin{bmatrix} 1 & 4\sigma & 2\sigma\sigma & 2\sigma\sigma\omega \\ 1 & 4a & 2\sigma b & 2\sigma\omega b \\ 1 & 4b & 2c & 2c\omega \\ 1 & 4b & 2c & 2c\omega \end{bmatrix} \quad (4)$$

Equation 4 can even be reduced to a 3×3 matrix, where

the indexing is now A, B, (C + D):

$$\mathbf{U}_{2nnd} = \begin{bmatrix} 1 & 4\sigma & 2\sigma\sigma(1+\omega) \\ 1 & 4a & 2\sigma b(1+\omega) \\ 1 & 4b & 2c(1+\omega) \end{bmatrix} \quad (5)$$

This further condensation is validated since it reproduces the same eigenvalues.

The values of the new parameters a , b , and c have to be determined so that the 4×4 , 4×2 , 2×4 , and 2×2 submatrices in eq 3 will weight the conformations of the chains on the 2nnd lattice so that they closely mimic the conformations of polyethylene. By using the geometric mean to calculate a , b , and c ,

$$a = \sigma\omega^{1/8}$$

$$b = \sigma\omega^{1/4}$$

$$c = \sigma^2\omega^{1/2}$$

we reproduced the expected dimensions of the chains (see the following). Even though the conformational probabilities of chains simulated in this manner also agreed well enough, considering the simplicity of the model, results shown in the following will point out that this recipe might not be of use for all kinds of polymers. To find a "universal" solution, this matter is investigated more fully in Appendix A. Generalization to other chains of the matrix in eq 2 is presented in Appendix B.

Defining the Probabilities for the Moves of 2nnd Lattice Chains. The implementation of the coarse-grained statistical weights introduced in the previous section is used here to calculate the probabilities of the single bead moves of the 2nnd lattice chains.

In the detailed (classical) RIS description, the probability for a specific conformation of a long chain with n pairwise interdependent bonds is given by $p_{\eta;2}$ and $q_{\xi\eta;i}$, $2 < i \leq n-1$, as²

$$p = P_{\alpha;2} q_{\alpha\beta;3} q_{\beta\gamma;4} q_{\gamma\delta;5} \cdots q_{\psi\omega;n-1} \quad (6)$$

where $p_{\eta;i}$ is the probability that bond i will be in state η , and $q_{\xi\eta;i}$ is the conditional probability that bond i will be in state η , given that bond $i-1$ is in state ξ . The $p_{\eta;i}$ and $q_{\xi\eta;i}$ are derived from the standard statistical weight matrix shown in eq 1. This definition of a chain probability p can easily be adapted to the conformation of a chain on the 2nnd lattice. Instead of n bonds in the detailed description, there are $N = n/2$ virtual bonds describing the corresponding chain on the 2nnd lattice. According to Figure 1, the probability of the chain described earlier uses the following conversions when changing to a chain on the 2nnd lattice. New and conditional probabilities, which are derivable from the extended, coarse-grained statistical weights, are denoted by $P_{\xi\eta;i}$ and $Q_{\xi\eta\zeta\kappa;i}$. These probabilities and conditional probabilities define vectors connecting beads i and $i+2$ on the 2nnd lattice. Thus, $P_{\xi\eta;i}$ defines the probability of the vector connecting beads 1 and 3 on the 2nnd lattice. This probability is defined by two states ξ and η in the detailed representation. Accordingly, $Q_{\xi\eta\zeta\kappa;2}$ defines the conditional probability of the vector connecting beads 2 and 4 on the 2nnd lattice. It is defined by the two states ζ and κ in the detailed representation, giving that the two previous states are ξ and η . The probability for the whole chain in terms of probabilities and conditional probabilities in the coarse-grained nota-

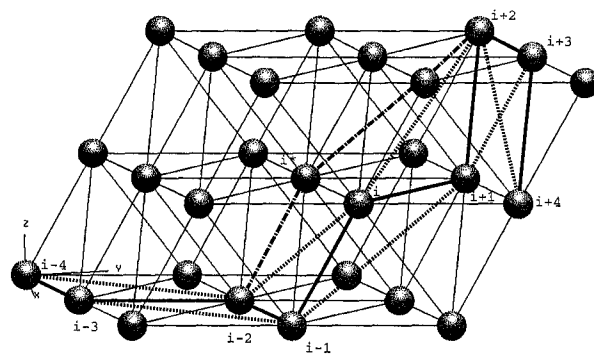


Figure 2. Change in local conformation when bead i is moved to bead i^* . The thick solid line represents the chain on the 2nnd lattice, and the dashed lines represent the types of corresponding conditional probabilities according to their length. The only two conditional probabilities affected by the move are the ones symbolized by the virtual bond vectors connecting beads $i-2$ and i and beads i and $i+2$, depicted as dash-dotted lines in the new conformation.

tion (derived from eq 3) then is

$$p = P_{\alpha\beta;1} Q_{\alpha\beta\gamma\delta;2} Q_{\gamma\delta\epsilon\zeta;3} \cdots Q_{\phi\chi\psi\omega;N-1} \quad (7)$$

By substituting the states of the detailed bonds with the states of the vectors connecting beads i and $i+2$ on the 2nnd lattice, $\bar{\alpha}$, $\bar{\beta}$, $\bar{\gamma}$, ..., according to the categorization presented in Table 1, the probability of the conformation of the chain then reads (by using the probabilities and conditional probabilities derived from eq 3 or 4)

$$p = P_{\bar{\alpha};1} Q_{\bar{\alpha}\bar{\beta};2} Q_{\bar{\beta}\bar{\gamma};3} \cdots Q_{\bar{\psi}\bar{\omega};N-1} \quad (8)$$

The probability of moving one bead is the probability of the new conformation divided by the probability of the old conformation. If the expression for the probability of a certain conformation is known, the probability of a certain move can easily be derived. Suppose we were moving bead i to bead i^* , then the only vectors changing would be the vectors connecting bead $i-2$ to bead i and bead i to bead $i+2$, as can easily be seen in Figure 2. The probability of the new conformation of the chain would be

$$p = P_{\bar{\alpha};1} Q_{\bar{\alpha}\bar{\beta};2} \cdots Q_{\bar{\zeta}^* \bar{\eta};i-2} Q_{\bar{\zeta}^* \bar{\eta};i-1} Q_{\bar{\eta} \bar{i}^*;i} Q_{\bar{i}^* \bar{\kappa};i+1} \cdots Q_{\bar{\psi}\bar{\omega};N-1} \quad (9)$$

where $\bar{\zeta}^*$ and \bar{i}^* represent the states of the vectors connecting beads $i-2$ and i^* and beads i^* and $i+2$, which are the vectors that changed conformation. The ratio of the probabilities for the new and old conformations within a chain reduces to

$$\frac{p_{\text{new}}}{p_{\text{old}}} = \frac{Q_{\bar{\zeta}^* \bar{\eta};i-2} Q_{\bar{\zeta}^* \bar{\eta};i-1} Q_{\bar{\eta} \bar{i}^*;i} Q_{\bar{i}^* \bar{\kappa};i+1}}{Q_{\bar{\zeta} \bar{\eta};i-2} Q_{\bar{\zeta} \bar{\eta};i-1} Q_{\bar{\eta} \bar{i};i} Q_{\bar{i} \bar{\kappa};i+1}} \quad (10)$$

provided that bead i is at least four beads removed from the nearest end of the chain.

The probability of a move of a bead within the chain is the Metropolis criterion:

$$p_{\text{move}} = \min \left[1, \frac{p_{\text{new}}}{p_{\text{old}}} \right] \quad (11)$$

which means that a move leading to a more probable conformation (or lower energy) is always accepted. A move leading to a less probable state (or higher energy)

is accepted only with the probability $p_{\text{new}}/p_{\text{old}}$, representing the Boltzmann weight of the increase in energy.

The formalism in eq 10 has to be modified slightly for moving the beads close to the ends of the chain. For moving the last bead, one has

$$\frac{p_{\text{new}}}{p_{\text{old}}} = \frac{Q_{\bar{\psi}\bar{\omega}^*;N-1}}{Q_{\bar{\psi}\bar{\omega};N-1}} \quad (12)$$

and for the first bead, we could write

$$\frac{p_{\text{new}}}{p_{\text{old}}} = \frac{P_{\bar{\alpha};1} Q_{\bar{\alpha}^*\bar{\beta};2}}{P_{\bar{\alpha};1} Q_{\bar{\alpha}\bar{\beta};2}} \quad (13)$$

However, by switching the direction for indexing the bonds along the chain, one could also formulate the probability of this move in the same way as the probability of moving the last bead. This would look like

$$\frac{p_{\text{new}}}{p_{\text{old}}} = \frac{Q_{\bar{\beta}\bar{\alpha}^*;1}}{Q_{\bar{\beta}\bar{\alpha};1}} \quad (14)$$

involving only the ratio of two conditional probabilities. For the second beads, one has

$$\frac{p_{\text{new}}}{p_{\text{old}}} = \frac{Q_{\bar{\alpha}\bar{\beta}^*;2} Q_{\bar{\beta}^*\bar{\gamma};3}}{Q_{\bar{\alpha}\bar{\beta};2} Q_{\bar{\beta}\bar{\gamma};3}} \quad (15)$$

and a similar expression for moving the second to the last bead. The probabilities of moving the third bead also involve $P_{\bar{\alpha}^*;1}$ and $P_{\bar{\alpha};1}$, which can be avoided by changing the ends of the chain. Therefore, one has

$$\frac{p_{\text{new}}}{p_{\text{old}}} = \frac{Q_{\bar{\delta}\bar{\gamma}^*;4} Q_{\bar{\gamma}^*\bar{\beta};3} Q_{\bar{\beta}\bar{\alpha}^*;2}}{Q_{\bar{\delta}\bar{\gamma};4} Q_{\bar{\gamma}\bar{\beta};3} Q_{\bar{\beta}\bar{\alpha};2}} \quad (16)$$

and of course a very similar expression for moving the third to the last bead of the chain.

In eqs 10–16, the probabilities for the moves of all beads were defined by using only the conditional probabilities of the coarse-grained model. Since even in the classical RIS description the end effects are rather small, they have been omitted from this representation.

Determination of the Conditional Probabilities. This section describes how the conditional probabilities for the coarse-grained model are determined. These conditional probabilities were used in the previous section to derive the probabilities for the moves.

The conditional probabilities are a simple modification of the probabilities of a certain state at a certain bond. For a classical RIS model with pairwise interdependent bonds, these probabilities have to be calculated for individual bonds and pairs of consecutive bonds. These probabilities can be defined as the ratio of the partition function, with the restriction of the specific bond(s), to the total partition function (using eq 1):²

$$p_{\eta;i} = Z_{\eta;i}/Z; \quad p_{\xi\eta;i}/Z \quad (17)$$

Accordingly, this formalism can be expanded to obtain the probabilities for four consecutive bonds in specific states (using eq 2):

$$p_{\zeta\kappa\xi\eta;i} = Z_{\zeta\kappa\xi\eta;i}/Z \quad (18)$$

For these calculations, one has to use the extended statistical weight matrix (eq 2) instead of the usual statistical weight matrix (eq 1). Use of the probabilities for four bonds as defined in eq 18 describes the chain statistics in exactly the same way as use of the probabilities for two bonds in eq 17. If one takes the coarse-grained statistical weight matrix (eq 3) to calculate the probabilities (eq 18), the only approximation is the effect due to the coarse-grained statistical weights. The probabilities and chain statistics are not affected by using a 9×9 statistical weight matrix instead of the 3×3 statistical weight matrix for the classical RIS description. The probabilities for the coarse-grained description, using eqs 3 and 4, are defined as

$$P_{\zeta\kappa\xi\eta;i} = Z_{\zeta\kappa\xi\eta;i}/Z \quad \text{or} \quad P_{\xi\eta;i} = Z_{\xi\eta;i}/Z \quad (19)$$

The conditional probabilities are obtained as a simple renormalization of the rows of the matrix $\mathbf{P}_{\zeta\kappa\xi\eta;i}$ (or $\mathbf{P}_{\xi\eta;i}$) containing the elements $P_{\zeta\kappa\xi\eta;i}$ (or $P_{\xi\eta;i}$). While all elements in $\mathbf{P}_{\xi\eta;i}$ and $\mathbf{P}_{\zeta\kappa\xi\eta;i}$ add to 1, all elements of each row of $\mathbf{Q}_{\xi\eta;i}$ and $\mathbf{Q}_{\zeta\kappa\xi\eta;i}$ add to 1. This requirement is necessary since the probability of all possible states of the virtual bond vectors connecting beads i and $i+2$ must add to 1 for every state of the virtual bond vector connecting beads $i-1$ and $i+1$.

A numerical example of the matrix of the conditional probabilities in the detailed form $\mathbf{Q}_{\zeta\kappa\xi\eta;i}$ for polyethylene at 300 K, using $\sigma = 0.430\,889$ and $\omega = 0.034\,472$, is

$$\mathbf{Q}_{\zeta\kappa\xi\eta;i} = \begin{bmatrix} 0.39 & 0.13 & 0.13 & 0.13 & 0.13 & 0.046 & 0.046 & 0.0016 & 0.0016 \\ 0.51 & 0.11 & 0.11 & 0.11 & 0.11 & 0.026 & 0.026 & 0.00088 & 0.00088 \\ 0.51 & 0.11 & 0.11 & 0.11 & 0.11 & 0.026 & 0.026 & 0.00088 & 0.00088 \\ 0.51 & 0.11 & 0.11 & 0.11 & 0.11 & 0.026 & 0.026 & 0.00088 & 0.00088 \\ 0.51 & 0.11 & 0.11 & 0.11 & 0.11 & 0.026 & 0.026 & 0.00088 & 0.00088 \\ 0.62 & 0.088 & 0.088 & 0.088 & 0.088 & 0.013 & 0.013 & 0.00046 & 0.00046 \\ 0.62 & 0.088 & 0.088 & 0.088 & 0.088 & 0.013 & 0.013 & 0.00046 & 0.00046 \\ 0.62 & 0.088 & 0.088 & 0.088 & 0.088 & 0.013 & 0.013 & 0.00046 & 0.00046 \\ 0.62 & 0.088 & 0.088 & 0.088 & 0.088 & 0.013 & 0.013 & 0.00046 & 0.00046 \end{bmatrix} \quad (20)$$

and in the condensed form $\mathbf{Q}_{\xi\eta;i}$, which can be used to calculate the probabilities of the moves as described earlier, is

$$\mathbf{Q}_{\xi\eta;i} = \begin{bmatrix} 0.69 & 0.23 & 0.080 & 0.0028 \\ 0.79 & 0.17 & 0.040 & 0.0014 \\ 0.86 & 0.12 & 0.019 & 0.00064 \\ 0.86 & 0.12 & 0.019 & 0.00064 \end{bmatrix} \quad (21)$$

Note that the elements in eq 21 are taken as the individual elements of the indicated regions of eq 20 (rather than the sum of all elements in that row in the indicated region) and afterward renormalized for each row (see Appendix C).

Verification of the Short Range Interactions. This section describes the verification of the adaption of the short range interactions from the atomistic, detailed description of the polymer chain to the corresponding 2nd lattice chain. These short range interactions were introduced as a coarse-grained version of the classical RIS statistical weights.

Single-chain simulations on the 2nd lattice representing RIS polyethylene chains were set up by using only the described short range interactions. These simulations have the same excluded volume restrictions as defined by the nonreversal random walk. The simulations were performed for chain lengths of $N = 5, 9, 17, 33$, and 65 . The beads that were moved were

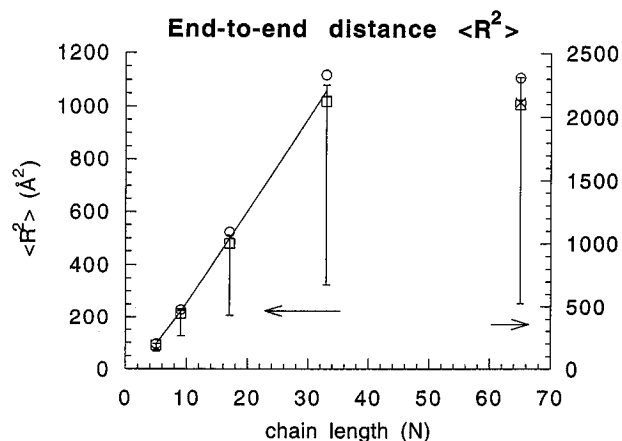


Figure 3. Mean-squared end-to-end distance as a function of the number of virtual bonds. The solid line on the left-hand side (for $N \leq 33$) and the point marked with an \times on the right-hand side (for $N = 65$) represent averages of R^2 in the simulations. Points marked with \circ and \square represent the mean-squared end-to-end distances for the RIS polyethylene chains determined by using the generator matrix method, with $\theta = 112^\circ$ and 109.5° , respectively. The error bars below the simulation points represent the width of the distribution for R^2 , and the error bars above the simulation points represent the accuracy of these points (see text).

chosen randomly, and the possible position(s) of the moved beads was uniquely determined as described previously.¹ The probabilities for the moves were calculated according to eqs 10, 12, and 14–16. The moves then were accepted by using the Metropolis criterion in eq 11. As mentioned earlier, the conditional probabilities were calculated by using the RIS energies $E_v = 0.5$ kcal/mol and $E_w = 2.0$ kcal/mol. The temperature was taken as 300 K, and the simulation length was taken as 11×10^6 Monte Carlo steps (MCS). A MCS is the simulation length where each bead has attempted to move once, on average. At the beginning of each run, 1×10^6 MCS were discarded to achieve a good equilibrium not influenced by the initial structures. (The simulation length for the longer chains had to be increased to 60×10^6 MCS for $N = 17$ and 95×10^6 MCS for $N = 33$ and 65, with equilibration times of 5×10^6 MCS.) The acceptance rate for these simulations was between 20.0% for $N = 5$ and 12.4% for $N = 65$. The mean-squared end-to-end distance of the chains is shown in Figure 3 as a solid line for $N \leq 33$ and as the point marked with an \times for $N = 65$. Points marked with a circle or square represent the mean-squared end-to-end distances for the RIS polyethylene chains determined by using the generator matrix method, with $\theta = 112^\circ$ and 109.5° , respectively. The error bars below the simulation points represent the standard deviation of R^2 for the whole simulation and are a measure of the width of the distribution of R^2 . In Figure 4, the distribution of R^2 for the chain lengths $N = 17$, 33, and 67 is shown as the fraction vs normalized dimension ($R^2/\langle R^2 \rangle$).

To estimate the accuracy of these simulations, the total length was divided into 10 subruns. For each subrun the average for R^2 was calculated. Of course, averaging of these averages resulted in the value obtained from the total simulation. The accuracy of the simulation was taken as the standard deviation of the averages of these 10 subruns. The error bars above the simulation points in Figure 3 denote this measure of the accuracy of the simulation. The average values for the simulated R^2 lie between the values calculated for

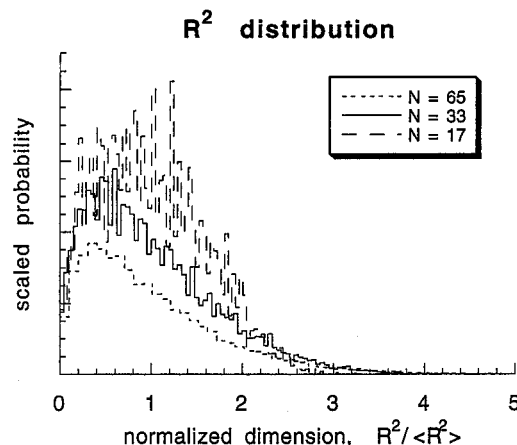


Figure 4. Distribution of the squared end-to-end distances for chain lengths $N=17$, 33, and 67. The x -axis shows the square of the end-to-end distance normalized with respect to the average value. To avoid overlaps, the values of the scaled probability for $N = 33$ have been multiplied by 1.5, and the values for $N = 17$ have been multiplied by 2.0.

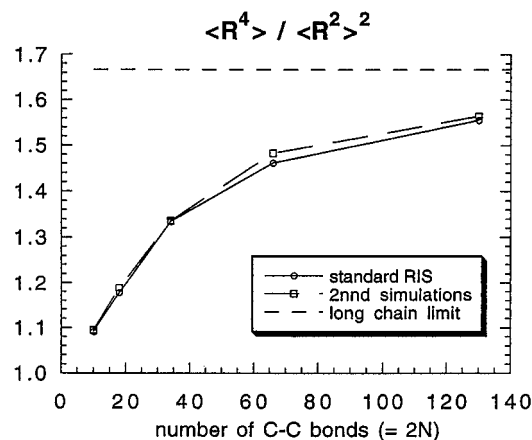


Figure 5. Comparison of the ratio $\langle R^4 \rangle / \langle R^2 \rangle^2$ for the standard RIS description and 2nnd lattice simulations.

RIS polyethylene with $\theta = 109.5^\circ$ and 112° . This result shows that the RIS polyethylene chain can be accurately mapped onto the 2nnd lattice.

The accuracy of the width of the distribution for R^2 was assessed by calculation of the dimensionless ratio $\langle R^4 \rangle / \langle R^2 \rangle^2$ and comparison to the values expected from the standard RIS model using generator matrices. This comparison, shown in Figure 5, demonstrates that the breadth of the distribution of R^2 is also well-reproduced in the simulations on the 2nnd lattice.

Another check of the validity of the short range interactions on the 2nnd lattice is the temperature dependence of the mean-square end-to-end distances. The simulations for the chain lengths mentioned earlier were additionally performed for four different temperatures, ranging from 294 to 306 K in steps of 3 K. The temperature dependence expressed as $(\partial \ln \langle R^2 \rangle / \partial T)_\infty$ is experimentally determined as $-1.1 \times 10^{-3} \text{ deg}^{-1}$ for very long chains at temperatures in the range of 110–190 $^\circ\text{C}$.⁴ This value can be reproduced nicely by using the standard RIS model with the indicated energies for E_v and E_w . The temperature coefficient at 300 K has been calculated by using the standard RIS model and is $-1.1 \times 10^{-3} \text{ deg}^{-1}$ for long chains. The simulation results, depicted in Figure 6, partially agree with this experimental value. For $N = 5$ and 9, the error bars, representing the accuracy of the average values as described earlier, are hardly visible. For these two

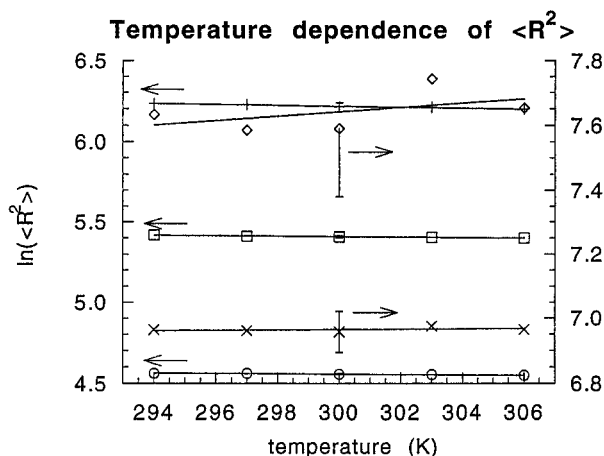


Figure 6. End-to-end distances as a function of temperature and chain length. The y-axis is logarithmic and provides the temperature dependence as the slope for the simulations at different temperatures. The chain lengths are symbolized by as follows: \circ , $N=5$; \square , $N=9$; $+$, $N=17$; \times , $N=33$; \diamond , $N=65$. At the values for 300 K there are error bars representing the accuracy, as previously defined for the end-to-end distances.

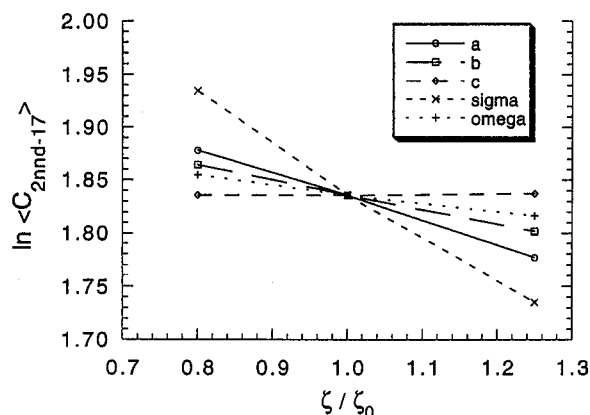


Figure 7. Influence of the variation in the different statistical weights on the dimensions of the chains at 300 K. The chain length was 17 virtual bonds on the 2nd lattice.

cases, the averages lie nicely on the linear fit, and the slopes of -1.1×10^{-3} and $-1.4 \times 10^{-3} \text{ deg}^{-1}$ are a little too small. For $N=17$, the error bar becomes clearly visible and the simulation points still lie nicely on the fitted line, but the temperature dependence has increased to $-2 \times 10^{-3} \text{ deg}^{-1}$. For chain lengths of $N=33$ and 65 , the error bars are much larger than the variation in the dimension itself, so that no reasonable deduction can be made for the temperature coefficients of these chain lengths.

Dependence of the Chain Dimensions on the Statistical Weights. To address the influence of the variation in the statistical weights, additional simulations were performed, each time varying only one statistical weight, σ or ω . The coarse-grained statistical weights a , b , and c were also changed when σ and ω were altered, because they are calculated as a function of σ and ω . The change in the dimensions was monitored as the change in $\ln C_N$ for the chain length $N=17$, where C_N is the characteristic ratio defined as $\langle R^2 \rangle / NL^2$. The statistical weights were changed to 80% and 125% of their original values, respectively. The behavior is depicted in Figure 7, where ζ represents the statistical weights σ , ω , a , b , and c , respectively. The dimensions are most sensitive to variation in σ , which is reasonable because it is the only statistical weight

Table 2. Influence of the Variation in the Statistical Weights on the Dimensions of the Chains with $N=17$ on the 2nd Lattice

| temperature (K) | $\partial \ln C / \partial \zeta$ | | | | |
|-----------------|-----------------------------------|----------|--------|--------|-------|
| | σ | ω | a | b | c |
| 290 | -0.464 | -0.0774 | -0.239 | -0.130 | 0.022 |
| 300 | -0.441 | -0.0848 | -0.226 | -0.139 | 0.037 |
| 310 | -0.431 | -0.0910 | -0.212 | -0.139 | 0.011 |

for a first-order interaction. Of the new parameters (a , b , and c) introduced during the mapping onto the 2nd lattice, the dimensions are most sensitive to a and least sensitive to c . This result is also reasonable, because a weights the relatively common $(tg)(gt)$ combinations, whereas c weights the relatively improbable $(g^+g^-)(g^-g^+)$ combinations.

The influence of the variation in the statistical weights upon the temperature coefficient was also investigated for additional temperatures 290 and 310 K. The results for all three temperatures are shown in Table 2. Variation in σ had the biggest influence on the temperature coefficient, ranging from -1.85×10^{-3} ($\sigma = 0.80\sigma_0$) to $-2.59 \times 10^{-3} \text{ deg}^{-1}$ ($\sigma = 1.25\sigma_0$).

Further Confirmation of the Mapping of the 2nd Lattice Chains. (a) Rings. The ratio between the dimensions for a chain forming a ring vs the linear chain of the same length is expressed as $\langle s^2 \rangle_{0,\text{ring}} / \langle s^2 \rangle_{0,\text{linear}}$, where s^2 denotes the squared radius of gyration. This ratio should approach 0.5 as $n \rightarrow \infty$.⁵ By using the chain length $N=65$, one obtains $\langle s^2 \rangle_{0,\text{ring}} = 175 \text{ \AA}^2$ and $\langle s^2 \rangle_{0,\text{linear}} = 337 \text{ \AA}^2$, which results in $\langle s^2 \rangle_{0,\text{ring}} / \langle s^2 \rangle_{0,\text{linear}} = 0.52$. This result is already very close to the expected value for the long chain limit.

(b) Using Different Sets of Statistical Weights. The main part of this paper concerns the development of the mapping procedure for RIS chains onto the 2nd lattice. Polyethylene was chosen as the example and is explained in detail. As a short consideration on the side, the dimensions for a few chains with different statistical weights (conformational energies) were investigated. We were interested to determine whether the dimensions of the 2nd lattice chains still compare well with the dimensions of RIS chains for other values of the statistical weights. In Table 3, the dimensions of chains with five different combinations of conformational energies are shown, along with the dimensions for polyethylene introduced earlier. These data show that the dimensions in most of the cases turn out to be too small for the chains on the 2nd lattice, compared to the corresponding RIS chains. The correspondence is most accurate for the statistical weight that represents polyethylene and is about 20–30% off for the other examples.

Since most real chains have $\omega < 1$, it is worthwhile to give special consideration to the three chains in Table 3 for which $E_\omega > 0$. Here we see that the accuracy of the mapping decreases as the mean-square dimension decreases. The accuracy also decreases as the probability of the *trans* conformations, p_t , decreases. The values of p_t calculated by using the RIS model are 0.64, 0.51, and 0.27 for chains 1, 3, and 6, respectively. This observation may be associated with the fact that the new coarse-grained statistical weights a , b , and c are associated with detailed local conformations in which at least half of the bonds are in *gauche* states. These results show that although the trends of the dimensions are reproduced correctly within the indicated uncertainties, a fine tuning of the procedure of the coarse graining

Table 3. Dimensions of Chains on the 2nnd Lattice Using Different Combinations of the Conformational Energies

| no. | E_o^a | E_w^a | $\langle R^2 \rangle$, 2nnd lattice ^b | $\langle R^2 \rangle^{b,c}$ | $\langle R^2 \rangle^{b,d}$ | accuracy ^e |
|----------------|---------|---------|---|-----------------------------|-----------------------------|-----------------------|
| 1 ^f | 2.1 | 8.4 | 2116 | 2099 | 2311 | 1.008 |
| 2 | 2.1 | 0.0 | 910.1 | 1124 | 1233 | 0.810 |
| 3 | 1.0 | 2.0 | 986.0 | 1221 | 1343 | 0.808 |
| 4 | 2.0 | -2.0 | 487.5 | 559.5 | 609.8 | 0.871 |
| 5 | -2.0 | -2.0 | 218.9 | 167.9 | 183.9 | 1.304 |
| 6 | -2.0 | 2.0 | 495.7 | 707.8 | 777.4 | 0.700 |

^a Energies in kilojoules/mole. ^b Distances in angstroms. ^c RIS, with a bond angle of 109.5°. ^d RIS, bond with a bond angle of 112.0°. ^e Ratio of column 4 to column 5. ^f Polyethylene, as described earlier.

of the statistical weights, as indicated in Appendix A, is to be performed.

Long Range Interactions

We define the interactions between segments on the 2nnd lattice that are beyond the local conformational preferences described earlier as long range interactions. Therefore, the long range interactions apply between sites in the same chain that are three or more bonds apart and between all sites on different chains.

Since the final goal of this model is to describe bulk systems, a few points have to be considered. Use of the 2nnd lattice for the simulation of bulk polyethylene at experimental densities would mean that about 21% of the sites would be occupied. It therefore seems reasonable to define the long range potential as finite repulsive for sites that are one lattice unit apart (interactions between the indicated site and sites occupying the first shell). Sites that are two lattice units apart (sites occupying the second shell) consequently need an attractive part for the long range interaction. In the first approach, these two kinds of interactions will be the only ones considered.

For the definition of the two potential parameters, the lattice formulation of the second virial coefficient as

$$B_2 = 1/2(1 - q\mu) \quad (22)$$

was considered.⁶ The parameter q represents the lattice coordination number, and μ measures the strength of the interaction, which is defined as $\exp[-\omega_{ij}(kT)^{-1}] - 1$ (ω_{ij} is the potential of average force between segments i and j). In the current case, eq 22 had to be extended to

$$B_2 = 1/2(1 - q_1\mu_1 - q_2\mu_2) \quad (23)$$

to account for two different interaction potentials. The lattice coordination numbers for the 2nnd lattice are $q_1 = 12$ for nearest neighbors and $q_2 = 42$ for second nearest neighbors. μ_1 and μ_2 represent the strengths of the two corresponding interactions through the potentials ω_{1ij} and ω_{2ij} .

Definition of the second virial coefficient to be zero will give a relationship between ω_{1ij} and ω_{2ij} . This relationship provides the potentials that represent a single chain in a Θ solvent and that can also be used to simulate bulk structures. Unfortunately, this relationship is not unambiguous, and not every combination of ω_{1ij} and ω_{2ij} that satisfies the condition of $B_2 = 0$ represents a single chain in a Θ solvent. However, testing of various combinations of ω_{1ij} and ω_{2ij} should eventually simulate single chains with unperturbed dimensions. These dimensions are already known and

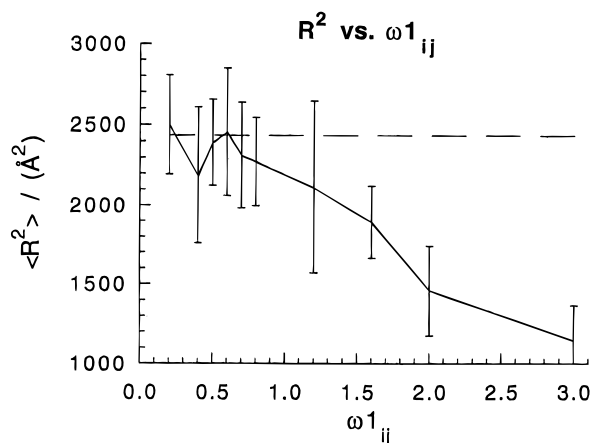


Figure 8. Dimensions of single chains ($N = 75$) as a function of ω_{1ij} . The values of ω_{2ij} are from eq 23, with $B_2 = 0$. The error bars show the accuracy as used in Figure 3. The dashed line represents the dimensions of the unperturbed (RIS) polymer chain (bond angle = 109.5°).

have been used in the verification of the short range interaction energies.

Single-chain simulations of chain length $N = 75$ were performed for ω_{1ij} in the range of 0.2–3.0 kJ/mol. The values of ω_{2ij} , specified by eq 23 with $B_2 = 0$, are -0.11 to -0.50 kJ/mol. The dimensions of the chains measured as the mean-square end-to-end distance are shown in Figure 8. These results suggest that values of the intermolecular potential of $\omega_{1ij} = 0.6$ kJ/mol and $\omega_{2ij} = -0.2$ kJ/mol will reproduce the dimensions of the Θ chain.

Acknowledgment. The authors thank Dr. G. Tanaka for discussions about the implementation of the long range interactions. This work was supported by Schweizerischer Nationalfonds zur Förderung der wissenschaftlichen Forschung and the National Science Foundation (Grant No. DMR 92-20369).

Appendix A. Toward a Rigorous Approach To Determine the Coarse-Grained Statistical Weights

Effort was undertaken to obtain coarse-grained statistical weights a , b , and c in a statistically derived, rigorous manner. The criteria of such a method are that simulations should provide the dimensions of the chains as well as the conformational probabilities in accordance with the applied RIS model. These criteria were achieved for polyethylene, but for different values of the statistical weights σ and ω the dimensions were not so well-reproduced as shown earlier.

By formulating the two bond probabilities as a function of the largest eigenvalue of the statistical weight matrix, one can set up a number of equations to determine a , b , and c . These equations for the general formulation of the statistical weight matrix \mathbf{U} for simple chains with a symmetric 3-fold rotation potential energy function,

$$\mathbf{U} = \begin{bmatrix} \tau & 2\sigma \\ 1 & \sigma(\psi + \omega) \end{bmatrix} \quad (A1)$$

are²

$$P_{ti,i} = \frac{\partial \ln \lambda_1}{\partial \ln \tau} \quad (A2)$$

$$p_{g^+;i} + p_{g^-;i} = \frac{\partial \ln \lambda_1}{\partial \ln \sigma} \quad (\text{A3})$$

$$p_{g^+g^+;i} + p_{g^-g^-;i} = \frac{\partial \ln \lambda_1}{\partial \ln \psi} \quad (\text{A4})$$

$$p_{g^+g^+;i} + p_{g^-g^+;i} = \frac{\partial \ln \lambda_1}{\partial \ln \omega} \quad (\text{A5})$$

where λ_1 is the largest eigenvalue of the matrix in eq A1.

A similar set of equations can be formulated for the statistical weight matrix shown in eq 5. If one sets the corresponding probabilities to be equal in the two formulations, this provides values for a , b , and c that ensure the correct probabilities of two successive bonds. Use of these values in the simulations, however, did not reproduce the dimensions of the chain, because the use of averages in a 9×9 statistical weight matrix necessarily introduces long range correlations. There seems to be no easy way to find a solution for a , b , and c that simultaneously reproduces the probabilities for two successive bonds and compensates for the long range correlation to provide the correct chain dimensions. This problem can be seen with the following argument: For reproducing the correct bond probabilities and chain dimensions, the statistical weights can be rescaled with factor f as²

$$\sigma_f = f\sigma, \quad \tau_f = f\tau, \quad \psi_f = \psi/f, \quad \omega_f = \omega/f \quad (\text{A6})$$

If one is not interested in a physically meaningful energy with a single statistical weight, this assumption can be made for an arbitrary f . Introduction of this scaling factor into the statistical weight matrix shown in eq 2 shows that there is unfortunately no value of f that will transform this equation into eq 3.

Of course there is always the possibility to develop a new RIS model with four torsional states in accordance with the statistical weight matrix $\mathbf{U}^{2'}$. This approach, however, would not fulfill our goal of providing a simple translation from existing models onto this new coarse-grained model. As a first approach we stay with the geometric mean to determine the coarse-grained statistical weights, especially since the results are satisfying for polyethylene. The quality of this approach will have to be validated in actual simulations by using RIS models for other polymer types that have the same general form of the statistical weight matrix (eq 5). The use of the geometric mean should be expected to give unsatisfactory results when applied to a chain for which a value of zero is assigned to one or more of the statistical weights for second-order interactions. The use of the geometric mean under these conditions would completely suppress certain conformations that should be allowed on the $2nnd$ lattice.

Appendix B. General Form for $\mathbf{U}_k^{(j)}$

The body of this article describes the construction of the conformation partition function for unperturbed linear polyethylene chains when they are mapped onto the $2nnd$ lattice, using two C–C bonds for each step on that lattice. The application was specific for the case where $j = 2$ ($j \equiv n/N$), with each C–C bond having the same 3×3 statistical weight matrix (eq 1). Here the method is generalized to chains in which different real covalent bonds may have different statistical weight matrices (as would be the case in macromolecules such

as poly(oxyethylene)), to chains in which the real covalent bonds do not all have the same number of rotational isomeric states (as would be the case in macromolecules such as poly(1,4-*trans*-butadiene) and poly(1,4-*cis*-butadiene)), and to the use of an arbitrary number of real covalent bonds for each step on the $2nnd$ lattice (meaning that the upper limit for j is unbounded). The approach is to first rewrite the result of the main body of the paper so that it can be used for any combination of numbers of rotational isomeric states and statistical weight matrices, but with $j = 2$ retained. Then specific equations are written for the cases where $j = 3$ and $j = 4$. Finally, the result is generalized to arbitrary j , $j > 1$.

General Form for $\mathbf{U}_k^{(j)}$ When $j = 2$. (a) Structure Considered. Five consecutive real bonds were considered, with indexes $i - 3$, $i - 2$, $i - 1$, i , and $i + 1$. The $2nnd$ chain has a bond k that spans real bonds $i - 2$ and $i - 1$ and a bond $k + 1$ that spans real bonds i and $i + 1$. The torsion angle at $2nnd$ bond k , denoted Φ_k , is determined by the torsions at real bonds $i - 1$ and i , denoted ϕ_{i-1} and ϕ_i , respectively. The numbers of states at real bonds $i - 1$ and i are denoted by v_{i-1} and v_i , respectively. In this appendix we do not require that $v_{i-1} = v_i$.

(b) Statistical Weight Matrices for the Real Bonds. The statistical weight matrix for real bond i is written (see ref 2, p 144) as

$$\mathbf{U}_i = \mathbf{V}_i \mathbf{D}_i \quad (\text{B1})$$

where \mathbf{V}_i is a $v_{i-1} \times v_i$ matrix that contains the statistical weights for the second-order interactions, and \mathbf{D}_i is a $v_i \times v_i$ diagonal matrix with the statistical weights for the first-order interactions on the main diagonal. For the special case of polyethylene that was treated in the body of the manuscript, $v_i = 3$ for $1 < i < n$:

$$\mathbf{D}_i = \text{diag}(1, \sigma, \sigma) \quad \text{for } 1 < i < n \quad (\text{B2})$$

$$\mathbf{V}_2 = \begin{bmatrix} 1 & 1 & 1 \\ 1 & 1 & 1 \\ 1 & 1 & 1 \end{bmatrix} \quad (\text{B3})$$

$$\mathbf{V}_i = \begin{bmatrix} 1 & 1 & 1 \\ 1 & 1 & \omega \\ 1 & \omega & 1 \end{bmatrix} \quad \text{for } 2 < i < n \quad (\text{B4})$$

(c) Statistical Weight Matrix for $2nnd$ Lattice Bond k . This statistical weight matrix, of dimensions $v_{i-3}v_{i-2} \times v_{i-1}v_i$, is denoted $\mathbf{U}_k^{(2)}$. It is generated from the preceding matrices as

$$\mathbf{U}_k^{(2)} = (\mathbf{C}_{i-3} \otimes \mathbf{V}_{i-1} \otimes \mathbf{R}_i) \mathbf{V}_i^D (\mathbf{D}_{i-1} \otimes \mathbf{D}_i) \quad (\text{B5})$$

where \mathbf{C}_i denotes a column of v_i elements, each element being 1; \mathbf{R}_i denotes a row of v_i elements, each element being 1; \mathbf{V}_i^D is a $v_{i-1}v_i \times v_{i-1}v_i$ diagonal matrix with the elements of \mathbf{V}_i listed along the main diagonal in reading order (see ref 2, p 147), and \otimes denotes the direct product. For the \mathbf{V}_i given in eq B4, $\mathbf{V}_i^D = \text{diag}(1, 1, 1, 1, \omega, 1, \omega, 1)$. Each bond may have a different \mathbf{V} , \mathbf{D} , and v in the formulation described in eq B5. Since the product of three matrices on the right-hand side of eq B5 employs two matrices that are diagonal, the result is independent of the sequence in which these three matrices are written.

When applied to polyethylene, this procedure generates $\mathbf{U}_k^{(2)}$ with the order of indexing for the rows and columns $tt, tg^+, tg^-, g^+t, g^+g^+, g^+g^-, g^-t, g^-g^+, g^-g^-$. The rows are indexed by the states at real C-C bonds $i-3$ and $i-2$, and the columns are indexed by the states at real C-C bonds $i-1$ and i . The matrix appearing in eq 2 has exchanged rows and columns as $5 \rightarrow 6, 6 \rightarrow 8, 7 \rightarrow 5, 8 \rightarrow 9$, and $9 \rightarrow 7$ to present it in blocked form. Thus, the matrix in eq 2 is

$$\mathbf{X}\mathbf{U}_k^{(2)}\mathbf{X}^T \quad (\text{B6})$$

with

$$\mathbf{X} = \begin{bmatrix} 1 & 0 & 0 & 0 & 0 & 0 & 0 & 0 & 0 \\ 0 & 1 & 0 & 0 & 0 & 0 & 0 & 0 & 0 \\ 0 & 0 & 1 & 0 & 0 & 0 & 0 & 0 & 0 \\ 0 & 0 & 0 & 1 & 0 & 0 & 0 & 0 & 0 \\ 0 & 0 & 0 & 0 & 0 & 0 & 1 & 0 & 0 \\ 0 & 0 & 0 & 0 & 1 & 0 & 0 & 0 & 0 \\ 0 & 0 & 0 & 0 & 0 & 0 & 0 & 0 & 1 \\ 0 & 0 & 0 & 0 & 0 & 1 & 0 & 0 & 0 \\ 0 & 0 & 0 & 0 & 0 & 0 & 0 & 1 & 0 \end{bmatrix} \quad (\text{B7})$$

The matrix \mathbf{X} may assume different forms for other chains. Its dimensions and composition depend on details such as the number of rotational isomeric states, the symmetry of the torsion potential energy function, whether or not the two ends of the subchain are intrinsically different, and the θ and ϕ for the rotational isomeric states.

General Form for $\mathbf{U}_k^{(j)}$ When $j = 3$. (a) Structure Considered. Seven consecutive real bonds were considered with indexes $i-4, i-3, i-2, i-1, i, i+1$, and $i+2$. The 2nnd chain has a bond k that spans real bonds $i-3, i-2$, and $i-1$ and a bond $k+1$ that spans real bonds $i, i+1$, and $i+2$.

(b) Statistical Weight Matrix for 2nnd Lattice Bond k . This statistical weight matrix is of dimensions $v_{i-4}v_{i-3}v_{i-2} \times v_{i-1}v_i v_{i+1}$. It is generated as

$$\mathbf{U}_k^{(3)} = (\mathbf{C}_{i-4} \otimes \mathbf{C}_{i-3} \otimes \mathbf{V}_{i-1} \otimes \mathbf{R}_i \otimes \mathbf{R}_{i+1}) \times (\mathbf{V}_i^D \otimes \mathbf{E}_{i+1})(\mathbf{E}_{i-1} \otimes \mathbf{V}_{i+1}^D)(\mathbf{D}_{i-1} \otimes \mathbf{D}_i \otimes \mathbf{D}_{i+1}) \quad (\text{B8})$$

where \mathbf{E}_i denotes the $v_i \times v_i$ identity matrix. For polyethylene, this procedure generates $\mathbf{U}_k^{(3)}$ with the order of indexing for the rows and columns $ttt, ttg^+, ttg^-, tg^+t, tg^+g^+, tg^+g^-, tg^-t, tg^-g^+, tg^-g^-, g^+tt, g^+tg^+, g^+tg^-, g^+g^+t, g^+g^+g^+, g^+g^+g^-, g^+g^-t, g^+g^-g^+, g^+g^-g^-, g^-tt, g^-tg^+, g^-tg^-, g^-g^+t, g^-g^+g^+, g^-g^+g^-, g^-g^-t, g^-g^-g^+, g^-g^-g^-$. The rows are indexed by the states at real bonds $i-4, i-3$, and $i-2$, and the columns are indexed by the states at real bonds $i-1, i$, and $i+1$. It may be convenient to interchange selected rows and columns to facilitate conversion to the blocked form.

General Form for $\mathbf{U}_k^{(j)}$ When $j = 4$. (a) Structure Considered. Nine consecutive real bonds were considered with indexes $i-5, i-4, i-3, i-2, i-1, i, i+1, i+2, i+3$. The 2nnd chain has a bond k that spans real bonds $i-4, i-3, i-2$, and $i-1$ and a bond $k+1$ that spans real bonds $i, i+1, i+2, i+3$.

(b) Statistical Weight Matrix for 2nnd Lattice Bond k . This statistical weight matrix is of dimensions $v_{i-5}v_{i-4}v_{i-3}v_{i-2} \times v_{i-1}v_i v_{i+1}v_{i+2}$. It is generated from the preceding matrices as

$$\mathbf{U}_k^{(4)} = \mathbf{A}\mathbf{B}_1\mathbf{B}_2\mathbf{B}_3\mathbf{B}_4 \quad (\text{B9})$$

where the first matrix on the right-hand side is given by

$$\mathbf{A} = \mathbf{C}_{i-5} \otimes \mathbf{C}_{i-4} \otimes \mathbf{C}_{i-3} \otimes \mathbf{V}_{i-1} \otimes \mathbf{R}_i \otimes \mathbf{R}_{i+1} \otimes \mathbf{R}_{i+2} \quad (\text{B10})$$

and the remaining matrices, all of which are diagonal, are

$$\mathbf{B}_1 = \mathbf{V}_i^D \otimes \mathbf{E}_{i+1} \otimes \mathbf{E}_{i+2} \quad (\text{B11})$$

$$\mathbf{B}_2 = \mathbf{E}_{i-1} \otimes \mathbf{V}_{i+1}^D \otimes \mathbf{E}_{i+2} \quad (\text{B12})$$

$$\mathbf{B}_3 = \mathbf{E}_{i-1} \otimes \mathbf{E}_i \otimes \mathbf{V}_{i+2}^D \quad (\text{B13})$$

$$\mathbf{B}_4 = \mathbf{D}_{i-1} \otimes \mathbf{D}_i \otimes \mathbf{D}_{i+1} \otimes \mathbf{D}_{i+2} \quad (\text{B14})$$

The rows are indexed by the states at real bonds $i-5, i-4, i-3$, and $i-2$, and the columns are indexed by the states at real bonds $i-1, i, i+1$, and $i+2$.

General Form for $\mathbf{U}_k^{(j)}$ When $j > 1$. (a) Structure Considered. $2j+1$ consecutive real bonds were considered with indexes $i-j-1, i-j, \dots, i+j-1$. The 2nnd chain has a bond k that spans real bonds $i-j, i-j+1, \dots, i-1$ and a bond $k+1$ that spans real bonds $i, i+1, \dots, i+j-1$.

(b) Statistical Weight Matrix for 2nnd Lattice Bond k . This statistical weight matrix is of dimensions $v_{i-j-1}v_{i-j} \dots v_{i-2} \times v_{i-1}v_i \dots v_{i+j-2}$. It is generated as

$$\mathbf{U}_k^{(j)} = \mathbf{A}\mathbf{B}_1\mathbf{B}_2 \dots \mathbf{B}_j \quad (\text{B15})$$

where the first matrix on the right-hand side is given by

$$\mathbf{A} = \mathbf{C}_{i-j-1} \otimes \mathbf{C}_{i-j} \otimes \dots \otimes \mathbf{C}_{i-3} \otimes \mathbf{V}_{i-1} \otimes \mathbf{R}_i \otimes \mathbf{R}_{i+1} \otimes \dots \otimes \mathbf{R}_{i+j-2} \quad (\text{B16})$$

and the remaining j matrices are diagonal. All but one of the diagonal matrices are constructed from one \mathbf{V}^D and $(j-1)\mathbf{E}$:

$$\mathbf{B}_1 = \mathbf{V}_i^D \otimes \mathbf{E}_{i+1} \otimes \mathbf{E}_{i+2} \otimes \dots \otimes \mathbf{E}_{i+j-2} \quad (\text{B17})$$

$$\mathbf{B}_2 = \mathbf{E}_{i-1} \otimes \mathbf{V}_{i+1}^D \otimes \mathbf{E}_{i+2} \otimes \dots \otimes \mathbf{E}_{i+j-2} \quad (\text{B18})$$

⋮

$$\mathbf{B}_{j-1} = \mathbf{E}_{i-1} \otimes \mathbf{E}_i \otimes \dots \otimes \mathbf{E}_{i+j-4} \otimes \mathbf{V}_{i+j-2}^D \quad (\text{B19})$$

The remaining diagonal matrix is constructed from j diagonal matrices \mathbf{D} .

$$\mathbf{B}_j = \mathbf{D}_{i-1} \otimes \mathbf{D}_i \otimes \dots \otimes \mathbf{D}_{i+j-2} \quad (\text{B20})$$

The rows of $\mathbf{U}_k^{(j)}$ are indexed by the states at real bonds $i-j-1, i-j, \dots$, and $i-2$, and the columns are indexed by the states at real bonds $i-1, i, \dots$, and $i+j-2$.

Appendix C. Remark on the Determination of the Conditional Probabilities

The conditional probabilities $\mathbf{Q}_{\tilde{\eta};p}$ as shown in eq 21, should also be derivable from the 4×4 matrix describing the coarse-grained RIS model, \mathbf{U}_{2nnd} (eq 4). Due to the differences in the multiplicity of the coarse-grained conformations and the method used for moving the

chain segments, careful considerations are necessary for the evaluation of the \mathbf{Q} 's to be used in eq 10.

The factors of 4 and 2 appear in the last three columns of the \mathbf{U}_{2nd} in eq 4 because of the multiplicity of detailed conformations represented by each element in these three columns. For example, the second element in the first row has the statistical weights for four detailed conformations (tg^+ , tg^- , g^+t , g^-t) following tt . Each of these detailed conformations contributes a statistical weight of σ , and the sum for all four conformations is 4σ .

However, the usage of the \mathbf{Q} 's in eq 10 is to evaluate the ratios of the probabilities of a single detailed new conformation and a single detailed old conformation. A sequence of four real bonds in a detailed conformation might be any of $tttg^+$, $tttg^-$, ttg^+t , or ttg^-t , but it cannot be all four of them simultaneously. Therefore, the desired \mathbf{Q} 's in eq 10 must be computed from a modified \mathbf{U}_{2nd} that chops the multiplicity of the conformations.

The $\mathbf{Q}_{\xi\eta,i}$ in eq 21 is obtained from

$$\begin{bmatrix} 1 & \sigma & \sigma\sigma & \sigma\sigma\omega \\ 1 & a & \alpha b & \sigma\omega b \\ 1 & b & c & c\omega \\ 1 & b & c & c\omega \end{bmatrix} \quad (\text{C1})$$

with the sum of elements in each row normalized to 1.

References and Notes

- (1) Rapold, R. F.; Mattice, W. L. *J. Chem. Soc., Faraday Trans.* **1995**, *91*, 2435.
- (2) Mattice, W. L.; Suter, U. W. *Conformational Theory of Large Molecules. The Rotational Isomeric State Model in Macromolecular Systems*; Wiley: New York, 1994.
- (3) Abe, A.; Jernigan, R. L.; Flory, P. J. *J. Am. Chem. Soc.* **1966**, *88*, 631.
- (4) Flory, P. J. *Statistical Mechanics of Chain Molecules*; Wiley: New York, 1969. Reprinted with the same title by Hanser: München (Münich), 1989.
- (5) Kramers, H. *J. Chem. Phys.* **1946**, *14*, 415.
- (6) Post, C. B.; Zimm, B. H. *Biopolymers* **1979**, *18*, 1487.

MA9513628